Molecular Crystals and Liquid Crystals
Publication details, including instructions for authors and subscription information:
http://www.tandfonline.com/loi/gmcl20

Synthesis of Symmetric Liquid Crystal Dimers Based on Azo and Imine Groups and Investigation of Phase Behaviour by Varying Alkoxy Terminal Chain Length

Tae Hyeong Kim [a], Chang Sin Lee [a], B. Ramaraj [a], Hye Jin Jeon [b], Hyun Hoon Song [b], Soo Min Lee [a] & Kuk Ro Yoon [a]

[a] Organic and Polymer Synthesis Laboratory, Chemistry Department, Hannam University, Daejeon, Korea

[b] Polymer Structural Physics Laboratory, Advanced Materials Department, Hannam University, Daejeon, Korea

Version of record first published: 31 Aug 2012.

Mol. Cryst. Liq. Cryst., Vol. 492, pp. 102/[466]–116/[480], 2008

ISSN: 1542-1406 print/1563-5287 online
DOI: 10.1080/15421400802331042

Synthesis of Symmetric Liquid Crystal Dimers Based on Azo and Imine Groups and Investigation of Phase Behaviour by Varying Alkoxy Terminal Chain Length

Tae Hyeong Kim[1], Chang Sin Lee[1], B. Ramaraj[1], Hye Jin Jeon[2], Hyun Hoon Song[2], Soo Min Lee[1], and Kuk Ro Yoon[1]
[1]Organic and Polymer Synthesis Laboratory, Chemistry Department, Hannam University, Daejeon, Korea
[2]Polymer Structural Physics Laboratory, Advanced Materials Department, Hannam University, Daejeon, Korea

With the objective to study the effect of alkoxy terminal chain length on mesomorphic properties of liquid crystals, we have synthesized two (Azo and Imine) different series of dimesogens by varying terminal alkoxy chain length (n = 6–12) with a short spacer unit in between two mesogens. Transition temperatures and phase characterization were studied by DSC, POM and XRD analysis. It was found that all the dimers show mesomorphic properties and the change in terminal alkoxy chain length has pronounced effect on the smectic phase window. In the DSC cooling scan, the smectic phase window of azo compounds increased from 6.4°C (2A$_6$) to 16.0°C(2A$_{12}$), whereas in Schiff base compounds, it increased from 9.2°C (2S$_6$) to 31.0°C(2S$_{12}$). Further, the 2A$_{11}$ dimer was found to undergo photo induced configurational changes.

Keywords: azobenzene; differential scanning calorimetry; liquid crystal; optical microscopy; Schiff's base; X-ray diffraction

1. INTRODUCTION

Liquid crystalline dimesogens (dimers) are attracting much attention because they exhibit variety of phases and serve as useful models for the semi-flexible, main-chain liquid crystal polymer [1–3]. In typical dimers where two individual mesogenic entities are attached to each

This research work was supported by Hannam University Research fund.
Address correspondence to Kuk Ro Yoon, Department of Chemistry, Hannam University, 133 Ojeong-Dong, Daedeuk-gu, Daejeon 306-791, Korea. E-mail: kryoon@hannam.ac.kr and Soo Min Lee, Organic and Polymer Synthesis Laboratory, Chemistry Department, Hannam University, Daejeon 305-811, Korea. E-mail: smlee@hnu.ac.kr

other via flexible polymethylene spacer units, the structure of the mesophases can be modified through the change in spacer length and terminal chain length. The mesomorphic behaviour of an organic compound is basically dependent on its molecular architecture in which a slight change in the molecular geometry brings about considerable change in its mesomorphic properties. Most of these studies have been focused on ester-Schiff's base and azo-dimers. Ester-Schiff's base dimers are known to exhibit room temperature nematic phase. Azo compounds are very attractive for their high thermal stability and for the photo-induced effects as well as for the potential applications in liquid crystal displays and devices, reversible optical storage systems, nonlinear optical waveguides, photo-refractive switches, and holographic gratings. Reversible optically induced switching effect has been the basis for these applications [4–8]. Precise placement of photochromic moieties within the liquid crystal dimesogen also could lead to reversible photo-induced configurational and constitutional changes [9]. Where as the schiff's bases is of particular interest since the discovery of 4-methoxy benzylidene-4′-butylaniline (MBBA), which exhibits a room temperature nematic phase [10].

We have recently reported the synthesis and mesomorphic properties of dimeric ester-Schiff bases (2ES-n) and azobenzenes ($2A_n$) series in order to explore the thermal stability of liquid crystals and the relationship with its molecular structures. These two series of the bent-shaped dimers have a polar hydroxyl group on the center of the short odd-numbered spacer, different terminal chains and mesogenic structure [11–13]. With the objective to explore, further, the effect of alkoxy terminal chain length on mesomorphic properties of liquid crystals, we have synthesized two; azo ($2A_n$) and Schiff's base ($2S_n$); different series of dimesogens by varying terminal alkoxy chain length (n = 6–12) with a short (-OCH_2CH_2 CH_2O-) spacer unit in between two mesogens. The chemical structures of these two series of mesogens were examined by Fourier transform infrared (FT-IR) spectroscopy and proton nuclear magnetic resonance (^{1}H NMR) spectroscopy. The mesomorphic properties and optical textures of the resultant dimers were investigated by differential scanning calorimetry (DSC), polarized optical microscopy (POM) and X-ray diffraction (XRD).

2. EXPERIMENTAL

2.1. Materials

4-Hydroxynitrobenzene, 1,3-bromopropane, hydrazine monohydrate, palladium on activated carbon (Pd/C, 10%), 1-bromoalkane (1-bromohexane,

1-bromoheptane, 1-bromooctane, 1-bromononane, 1-bromodecane, 1-bromoundecane, 1-bromododecane), p-toluenesulfonic acid (PTSA), anhydrous ethanol were purchased from Aldrich Chemical Co. and used as received. All other solvents and reagents were purchased commercially and used.

2.2. Synthesis

2.2.1. Synthesis of Azo ($2A_n$) Dimesogens

The $2A_n$ dimesogens were synthesized according to the method described in the literature [11,12,14] as illustrated in Scheme 1 and final products were structurally characterized by IR, ^{1}H NMR.

2.2.1.1. 1,3-Bis(4-(4-alkyloxyphenylazo)phenoxy)propane[$2A_n$]. The synthetic route used in the preparation of azo dimesogens involved four steps: (1) first the conventional etherification of 4-hydroxynitrobenzene with 1,3-dibromopropane in presence of potassium iodide and potassium carbonate to obtain 1,3-bis(4-nitrophenoxy)propane [BNPP], (2) then the reduction of nitro group with hydrazine

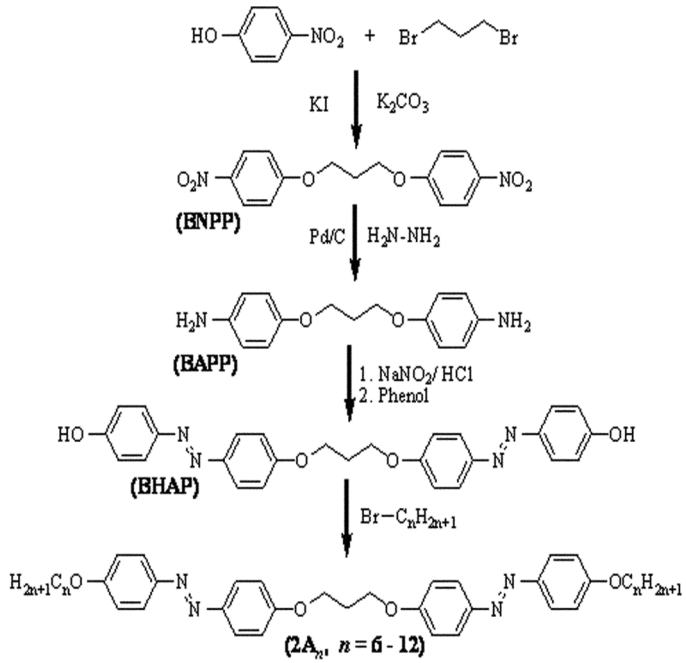

SCHEME 1 Synthetic pathway for azo dimesogens ($2A_n$).

monohydrate in the presence of palladium on activated carbon to obtain 1,3-bis(4-amiophenoxy)propane [BAPP], (3) the amine was then converted into its diazonium chloride and diazonium chloride on reaction with phenol forms 1,3-bis(4-(4-hydroxyphenylazo)phenoxy) propane [BHAP], (4) finally the BHAP reacted with different bromoalkanes (n = 6–12) to obtain the final products as per the procedure: BHAP (1.28 mmol) and K_2CO_3 (4.3 mmol) were dissolved in anhydrous ethanol (50 mL). 1-Bromoalkane (8.5 mmol) was added very slowly into the reaction mixture for about 30 min, and then the mixture was stirred for 20 h at the room temperature. The resulting precipitate was isolated by filtration and purified by the recrystallization from chloroform to obtain the final products (yellow solid, 87–95%). The IR and NMR data of final products are listed below.

$2A_6$: Yield, 90%. FT-IR (KBr pellet, cm^{-1}): 1580 (-N=N-). ^{1}H-NMR ($CDCl_3$, ppm): δ 0.90 (t, 6H, -CH_3), 1.31–1.51 (m, 12H, -$(CH_2)_3$-), 1.82 (m, 4H, -$\underline{CH_2}CH_2O$-), 2.35 (m, 2H, -$OCH_2\underline{CH_2}CH_2O$-), 4.03, (t, 4H, -$CH_2\underline{CH_2}O$-), 4.27 (t, 4H, -$O\underline{CH_2}CH_2\underline{CH_2}O$-), 6.62–6.65 (dd, 8H, Ar-H), 7.85–7.89 (d, 8H, Ar-H).

$2A_7$: Yield, 87%. FT-IR (KBr pellet, cm^{-1}): 1579 (-N=N-). ^{1}H-NMR ($CDCl_3$, ppm): δ 0.90 (t, 6H, -CH_3), 1.31–1.51 (m, 16H, -$(CH_2)_4$-), 1.82 (m, 4H, -$\underline{CH_2}CH_2O$-), 2.35 (m, 2H, -$OCH_2\underline{CH_2}CH_2O$-), 4.03, (t, 4H, -$CH_2\underline{CH_2}O$-), 4.27 (t, 4H, -$O\underline{CH_2}CH_2\underline{CH_2}O$-), 6.62–6.65 (dd, 8H, Ar-H), 7.85–7.89 (d, 8H, Ar-H).

$2A_8$: Yield, 91%. FT-IR (KBr pellet, cm^{-1}): 1580 (-N=N-). ^{1}H-NMR ($CDCl_3$, ppm): δ 0.89 (t, 6H, -CH_3), 1.31–1.51 (m, 20H, -$(CH_2)_5$-), 1.82 (m, 4H, -$\underline{CH_2}CH_2O$-), 2.35 (m, 2H, -$OCH_2\underline{CH_2}CH_2O$-), 4.03, (t, 4H, -$CH_2\underline{CH_2}O$-), 4.27 (t, 4H, -$O\underline{CH_2}CH_2\underline{CH_2}O$-), 6.62–6.65 (dd, 8H, Ar-H), 7.85–7.89 (d, 8H, Ar-H).

$2A_9$: Yield, 91%. FT-IR (KBr pellet, cm^{-1}): 1580 (-N=N-). ^{1}H-NMR ($CDCl_3$, ppm): δ 0.88 (t, 6H, -CH_3), 1.25–1.50 (m, 24H, -$(CH_2)_6$-), 1.82 (m, 4H, -$\underline{CH_2}CH_2O$-), 2.35 (m, 2H, -$OCH_2\underline{CH_2}CH_2O$-), 4.03, (t, 4H, -$CH_2\underline{CH_2}O$-), 4.27 (t, 4H, -$OCH_2CH_2\underline{CH_2}O$-), 6.97–7.04 (dd, 8H, Ar-H), 7.85–7.89 (d, 8H, Ar-H).

$2A_{10}$: Yield, 93%. FT-IR (KBr pellet, cm^{-1}): 1580 (-N=N-). ^{1}H-NMR ($CDCl_3$, ppm): δ 0.88 (t, 6H, -CH_3), 1.25–1.50 (m, 28H, -$(CH_2)_7$-), 1.82 (m, 4H, -$\underline{CH_2}CH_2O$-), 2.35 (m, 2H, -$OCH_2\underline{CH_2}CH_2O$-), 4.03, (t, 4H, -$CH_2\underline{CH_2}O$-), 4.27 (t, 4H, -$O\underline{CH_2}CH_2\underline{CH_2}O$-), 6.97–7.04 (dd, 8H, Ar-H), 7.85–7.89 (d, 8H, Ar-H).

$2A_{11}$: Yield, 95%. FT-IR (KBr pellet, cm^{-1}): 1579 (-N=N-). ^{1}H-NMR ($CDCl_3$, ppm): δ 0.88 (t, 6H, -CH_3), 1.25–1.50 (m, 32H, -$(CH_2)_8$-), 1.82 (m, 4H, -$\underline{CH_2}CH_2O$-), 2.35 (m, 2H, -$OCH_2\underline{CH_2}CH_2O$-), 4.03, (t, 4H, -$CH_2\underline{CH_2}O$-), 4.27 (t, 4H, -$O\underline{CH_2}CH_2\underline{CH_2}O$-), 6.97–7.04 (dd, 8H, Ar-H), 7.85–7.89 (d, 8H, Ar-H).

$2A_{12}$: Yield, 95%. FT-IR (KBr pellet, cm^{-1}): 1580 (-N=N-). ^{1}H-NMR ($CDCl_3$, ppm): δ 0.88 (t, 6H, $-CH_3$), 1.25–1.50 (m, 36H, $-(CH_2)_9-$), 1.82 (m, 4H, $-\underline{CH_2}CH_2O-$), 2.35 (m, 2H, $-OCH_2\underline{CH_2}CH_2O-$), 4.03, (t, 4H, $-CH_2\underline{CH_2}O-$), 4.27 (t, 4H, $-O\underline{CH_2}CH_2\underline{CH_2}O-$), 6.97–7.04 (dd, 8H, Ar-H), 7.85–7.89 (d, 8H, Ar-H).

2.2.2. Synthesis of Schiff Base ($2S_n$) Dimesogens

The $2S_n$ dimesogens were synthesized according to the method described in the literature [11,12,14] as illustrated in Scheme 2 and final products were structurally characterized by IR and ^{1}H NMR.

2.2.2.1. 1,3-Bis[4-((4-alkyloxyphenylimino)methyl)phenoxy]-propane [$2S_n$]. The synthetic route used in the preparation of Schiff base dimesogen series also involved four steps: (1) conventional etherification of 4-nitrophenol with an alkyl halide ($n = 6–12$) to produce the 4-alkoxynitrobenzenes (ANBn), (2) then reduction of nitro group with hydrazine monohydrate to produce 4-alkoxyanilines (AAn), (3) reaction of 4-hydroxybenzaldehyde (2 eq.) with 1,3-dibromopropane (1 eq.) to produce 1,3-bis(4-formylphenoxy)-propane (FPP-4), and (4) finally condensation reactions of FPP-4 with AAn yield the diimine compounds as per the details; 1,3-bis(4-formylphenoxy) propane

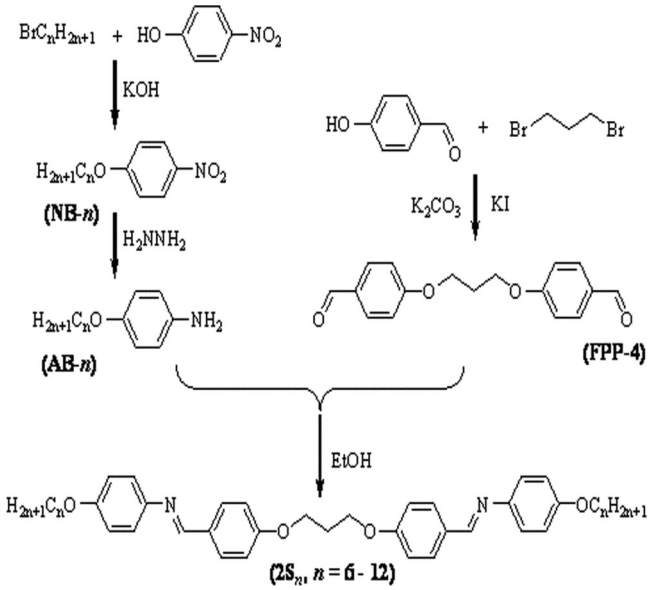

SCHEME 2 Synthetic pathway for Schiff base dimesogens ($2S_n$).

(FPP-4) (1.6 mmol) was dissolved in anhydrous ethanol (50 mL). 4-Alkyloxyaminobenzene (3.2 mmol) and a catalytic quantity of PTSA were mixed and stirred for 20 h at the room temperature. The resulting precipitate was isolated by filtration and purified by the recrystallization from ethanol. Final products were obtained as white solid (60–83%). The IR and NMR data of final products are listed below.

$2S_6$: Yield, 80%. FT-IR (KBr pellet, cm^{-1}): 1508, 1604 (-CH=N-). ^{1}H-NMR ($CDCl_3$, ppm): δ 0.91 (t, 6H, -CH_3), 1.29–1.35 (m, 12H, -$(CH_2)_3$), 1.71 (m, 4H, -$\underline{CH_2}CH_2O$-), 2.33 (m, 2H, -$OCH_2\underline{CH_2}CH_2O$-), 3.97 (t, 4H, -$CH_2\underline{CH_2}O$-), 4.25 (t, 4H, -$O\underline{CH_2}CH_2\underline{CH_2}O$-), 6.93 (d, 4H, Ar-H), 7.01 (d, 4H, Ar-H), 7.18 (d, 4H, Ar-H), 7.81 (d, 4H, Ar-H), 8.40 (s, 2H, -N=CH-).

$2S_7$: Yield, 81%. FT-IR (KBr pellet, cm^{-1}): 1508, 1604 (-CH=N-). ^{1}H-NMR ($CDCl_3$, ppm): δ 0.90 (t, 6H, -CH_3), 1.25–1.32 (m, 16H, -$(CH_2)_4$), 1.81 (m, 4H, -$\underline{CH_2}CH_2O$-), 2.33 (m, 2H, -$OCH_2\underline{CH_2}CH_2O$-), 3.97 (t, 4H, -$CH_2\underline{CH_2}O$-), 4.25 (t, 4H, -$OCH_2CH_2\underline{CH_2}O$-), 6.93 (d, 4H, Ar-H), 7.01 (d, 4H, Ar-H), 7.18 (d, 4H, Ar-H), 7.81 (d, 4H, Ar-H), 8.41 (s, 2H, -N=CH-).

$2S_8$: Yield, 83%. FT-IR (KBr pellet, cm^{-1}): 1508, 1604 (-CH=N-). ^{1}H-NMR ($CDCl_3$, ppm): δ 0.89 (t, 6H, -CH_3), 1.27–1.46 (m, 20H, -$(CH_2)_5$), 1.79 (m, 4H, -$\underline{CH_2}CH_2O$-), 2.33 (m, 2H, -$OCH_2\underline{CH_2}CH_2O$-), 3.97 (t, 4H, -$CH_2\underline{CH_2}O$-), 4.25 (t, 4H, -$O\underline{CH_2}CH_2\underline{CH_2}O$-), 6.93 (d, 4H, Ar-H), 7.01 (d, 4H, Ar-H), 7.18 (d, 4H, Ar-H), 7.81 (d, 4H, Ar-H), 8.40 (s, 2H, -N=CH-).

$2S_9$: Yield, 82%. FT-IR (KBr pellet, cm^{-1}): 1508, 1604 (-CH=N-). ^{1}H-NMR ($CDCl_3$, ppm): δ 0.89 (t, 6H, -CH_3), 1.28–1.46 (m, 24H, -$(CH_2)_6$), 1.79 (m, 4H, -$\underline{CH_2}CH_2O$-), 2.33 (m, 2H, -$OCH_2\underline{CH_2}CH_2O$-), 3.97 (t, 4H, -$CH_2\underline{CH_2}O$-), 4.25 (t, 4H, -$O\underline{CH_2}CH_2\underline{CH_2}O$-), 6.93 (d, 4H, Ar-H), 7.01 (d, 4H, Ar-H), 7.18 (d, 4H, Ar-H), 7.84 (d, 4H, Ar-H), 8.41 (s, 2H, -N=CH-).

$2S_{10}$: Yield, 72%. FT-IR (KBr pellet, cm^{-1}): 1510, 1604 (-CH=N-). ^{1}H-NMR ($CDCl_3$, ppm): δ 0.89 (t, 6H, -CH_3), 1.28–1.48 (m, 28H, -$(CH_2)_7$), 1.79 (m, 4H, -$\underline{CH_2}CH_2O$-), 2.33 (m, 2H, -$OCH_2\underline{CH_2}CH_2O$-), 3.97 (t, 4H, -$CH_2\underline{CH_2}O$-), 4.25 (t, 4H, -$O\underline{CH_2}CH_2\underline{CH_2}O$-), 6.93 (d, 4H, Ar-H), 7.01 (d, 4H, Ar-H), 7.18 (d, 4H, Ar-H), 7.81 (d, 4H, Ar-H), 8.40 (s, 2H, -N=CH-).

$2S_{11}$: Yield, 60%. FT-IR (KBr pellet, cm^{-1}): 1510, 1604 (-CH=N-). ^{1}H-NMR ($CDCl_3$, ppm): δ 0.88 (t, 6H, -CH_3), 1.27–1.48 (m, 32H, -$(CH_2)_8$), 1.79 (m, 4H, -$\underline{CH_2}CH_2O$-), 2.33 (m, 2H, -$OCH_2\underline{CH_2}CH_2O$-), 3.97 (t, 4H, -$CH_2\underline{CH_2}O$-), 4.25 (t, 4H, -$O\underline{CH_2}CH_2\underline{CH_2}O$-), 6.93 (d, 4H, Ar-H), 7.01 (d, 4H, Ar-H), 7.18 (d, 4H, Ar-H), 7.81 (d, 4H, Ar-H), 8.41 (s, 2H, -N=CH-).

$2S_{12}$: Yield, 77%. FT-IR (KBr pellet, cm^{-1}): 1508, 1604 (-CH=N-). ^{1}H-NMR ($CDCl_3$, ppm): δ 0.88 (t, 6H, $-CH_3$), 1.27–1.46 (m, 36H, $-(CH_2)_9$), 1.79 (m, 4H, $-\underline{CH_2}CH_2O-$), 2.33 (m, 2H, $-OCH_2\underline{CH_2}CH_2O-$), 3.97 (t, 4H, $-CH_2\underline{CH_2}O-$), 4.25 (t, 4H, $-O\underline{CH_2}CH_2\underline{CH_2}O-$), 6.93 (d, 4H, Ar-H), 7.01 (d, 4H, Ar-H), 7.18 (d, 4H, Ar-H), 7.81 (d, 4H, Ar-H), 8.40 (s, 2H, -N=CH-).

2.3. Characterization Methods

FT-IR spectra were recorded with a Perkin-Elmer 1000 FT-IR spectrophotometer on KBr pellets. ^{1}H NMR spectra were recorded by using a Varian Unity 300 (300 MHz) NMR spectrometer. DSC measurements were performed using a TA instrument 910S DSC apparatus under dry nitrogen flow at the heating rate of 10°C/min. The transition temperatures were taken at the maxima of peaks for each sample. Optical micrographs were obtained by using a Nikon Labophot-2 polarizing microscope fitted with a RTC-1 temperature controller (Instec Inc., Broomfield, Co.) and a Mettler FP-82HT hot stage. The UV irradiation was carried out by 10 mW/cm^2 UV lamp with a 365 nm peak wavelength. XRD measurements were performed at the 3C2 and 4C1 beamline in pohang Accelerator Laboratory.

3. RESULTS AND DISCUSSION

The synthetic routes used for the preparation of dimesogens (azo and imine group) are outlined in Scheme 1 and 2. The mesomorphic properties for these two ($2A_n$ & $2S_n$) series of dimesogens were determined by means of DSC, POM and XRD. DSC is a valuable aid by which phase transition temperature can be conveniently measured. This techniques offers a direct and complimentary (to microscopy) evaluation of thermal behaviour. Figure 1 presents the DSC heating and cooling traces of dimesogens ($2A_n$, $n = 6$–12). In the heating and cooling scans (Fig. 1), all the compounds in this series shows a crystal to smectic phase transition and a smectic to isotropic phase transition. The smectic phases are identified as smectic A on the basis of batonnets and broken fan textures observed when viewed through microscope. It can be seen from the Table 1, the crystal to smetic phase transition at 167.4°C ($2A_6$) decreased to 152.6°C ($2A_{12}$) with increase in chain length as expected; this clearly shows the dependence of thermal transition temperature on terminal chain length **n** of dimesogens for all $2A_n$ series. The heating scans of $n = 6$–9 show only a single melting transition temperature, but those of $n = 10$–12 showed smectic phases. In case of cooling scans, smectic phases are visible in all

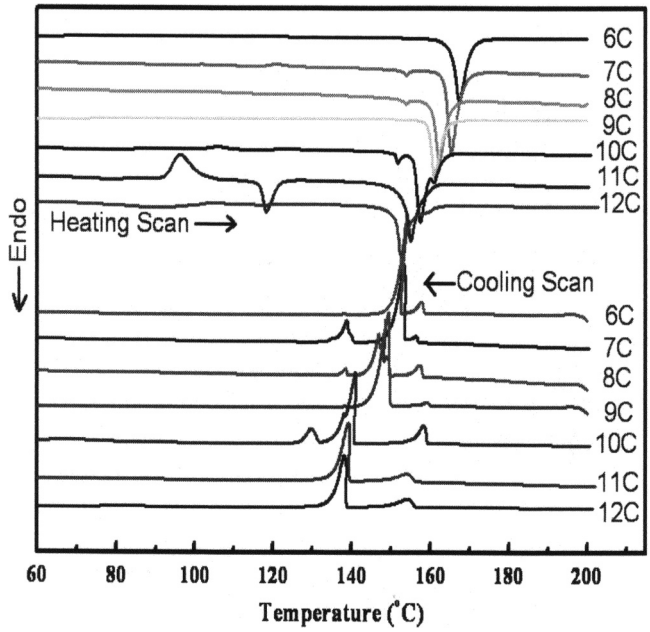

FIGURE 1 Differential scanning calorimetry thermograms for azo dimesogens ($2A_n$; n = 6–12) in the heating and cooling scans (10°C/min).

dimers (n = 6–12), where crystallization temperature decreased from 152.8°C (n = 6) to 138.0°C (n = 12). The smectic phase window is increased from 6.4°C (n = 6) to 16.0°C (n = 12). Since the molecules are bent-shaped dimesogens with two terminal chains, increasing the terminal chain length is anticipated to increase significantly the

TABLE 1 Thermal Transition Temperatures of Azo-Dimesogen ($2A_n$) Series Compounds

Number of carbons in $2A_n$ series	Heating cycle thermal transitions (°C)		Cooling cycle thermal transitions (°C)	
	Crystallization	Smectic	Crystallization	Smectic
6	167.4	–	152.8	159.2
7	165.3	–	152.0	156.4
8	162.2	–	151.5	157.3
9	161.0	–	149.5	157.8
10	157.4	161.1	141.0	158.4
11	156.2	161.0	139.3	153.9
12	152.6	160.9	138.0	154.0

length-to-breadth ratio in resulting liquid crystal phases, and particularly smectic phases, being stabilized at higher temperatures for higher homologues. We also note that the temperature range of the smectic mesophase increased with the terminal chain length. The compound of $2A_{12}$ shows the largest temperature interval extending to 16°C. These results demonstrate that the tendency toward smectic mesomorphism and the thermal stability of tilted smectic phase increased with increasing terminal alkoxy chain length. This may be the result of the terminal alkoxy chains lying at an angle to the long molecular axis inducing the molecular tilt between neighboring molecules. The effects of the terminal chain length on the transition temperatures and phases behavior observed in this series are in accordance with those observed for conventional low molar mass mesogens.

Optical micrographs of $2A_{11}$ and $2A_{12}$ obtained during the cooling cycle are shown in Figure 2. The micrograph of $2A_{11}$ exhibit batonnet texture at 142°C and crystal texture at 115°C, similarly the

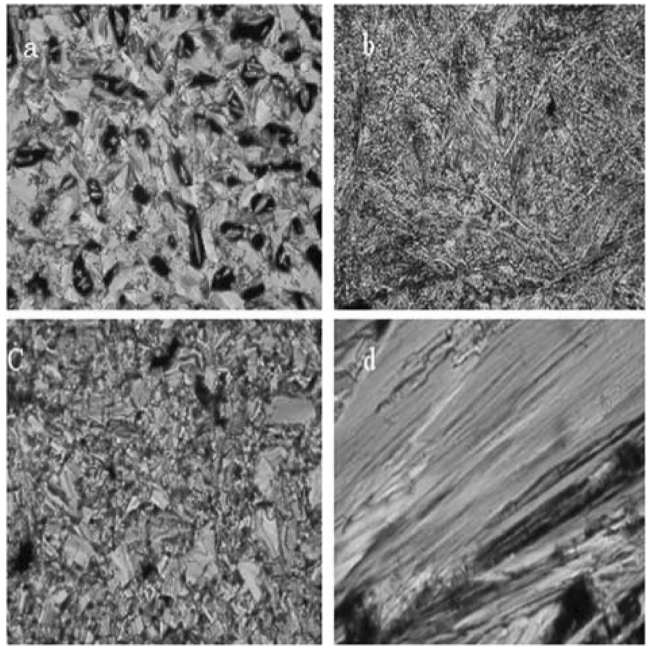

FIGURE 2 Optical photomicrographs of $2A_n$ (a) batonnets texture (Sm, cooling, 142°C), (b) crystal texture (Cr, cooling, 115°C) of $2A_{11}$ and (c) broken fan shape texture (Sm, cooling, 151°C), (d) crystal texture (Cr, cooling, 125°C) of $2A_{12}$ (10°C/min, $\times$ 100).

micrograph of $2A_{12}$ exhibit broken fan texture at 151°C and crystal texture at 125°C. Further analysis of the mesophases was performed with X-ray diffraction.

As a representative case of azo-dimesogens, an X-ray diffraction study was carried out on $2A_{12}$ to prove the presence of smectic phases beyond doubt. Figure 3 shows the X-ray diffractograms obtained at various temperatures for $2A_{12}$. At 118°C, it shows one sharp reflection in the small angle region and an array of small peaks in the wide angle regions corresponding to the formation of crystalline and various smectic phases. At higher temperatures, reflections corresponding to the smectic phases diffused, finally at 172°C, the crystalline phase also changes to isotropic liquid state. A clear change in the diffraction pattern of the sample could be observed. The sharp reflection in the small angle region confirms the formation of a highly ordered smectic A phase. In addition, small peaks, most probably a second order diffraction is seen in 118, 124, and 158°C diffractograms of the compound in the liquid crystalline phase.

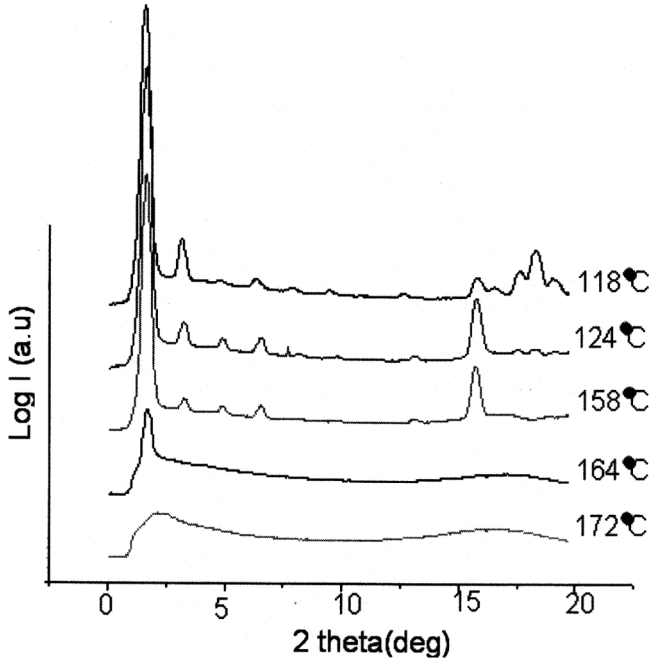

FIGURE 3 X-ray diffraction curves of azo-dimesogen ($2A_{12}$).

A reversible photochromic behavior of solution was evidenced when the sample $2A_{11}$ was exposed to UV irradiation. Dark incubation of a dichloromethane solution (50 μM/mL) of $2A_{11}$ has a maximum absorbance at 360 nm corresponding to the trans-azobenzene chromophore. Irradiation of this solution with 365 nm light resulted in photoisomerization to cis-$2A_{11}$, as evidenced by a decrease in the absorbance at 360 nm and an increase in absorbance at 451 nm and at 314 nm (Fig. 4). The stationary population of trans and cis isomers is a function of irradiation intensity. A photo stationary state from trans $2A_{11}$ to cis isomer was reached within approximately 50s under the irradiation at 365 nm.

New bent-shaped dimesogens, 1,3-bis(4-((4-alkyloxyphenylimino) methyl)phenoxy) propane ($2S_n$; n = 6–12), were synthesized starting from dialdehyde derivative, 1,3-bis(4-formylphenoxy)-propane (FPP-4). The dimesogens, $2S_n$, were then obtained by the condensation reaction between amines and dialdehyde (see Scheme 2). Figure 5 presents the DSC heating and cooling traces of dimesogens ($2S_n$, n = 6–12). In the heating and cooling scans, all the compounds in this

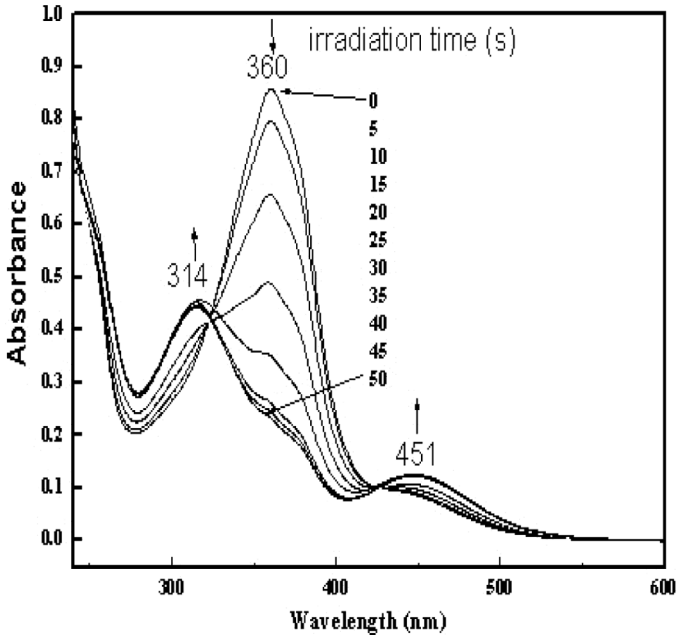

FIGURE 4 UV-VIS absorption spectra of $2A_{11}$ under irradiation (365 nm, at 0, 5, 10, 15, 20, 25, 30, 35, 40, 45, and 50 s).

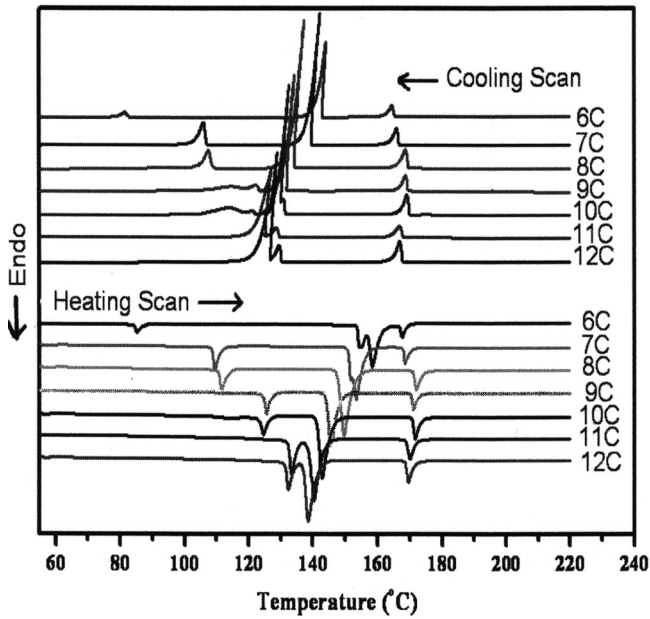

FIGURE 5 Differential scanning calorimetry thermograms for Schiff base dimesogens ($2S_n$; n = 6–12) in the heating and cooling scans (10°C/min).

series also shows a crystal to smectic phase transition and a smectic to isotropic phase transition. The thermal transition temperatures for dimesogens are summarized in Table 2. It can be seen from the Table 2, the crystal to smectic phase transition at 158.4°C ($2S_6$)

TABLE 2 Thermal Transition Temperatures of Schiff Base Dimesogen ($2S_n$) Series Compounds

Number of carbons in $2A_n$ series	Heating cycle thermal transitions (°C)		Cooling cycle thermal transitions (°C)	
	Crystallization	Smectic	Crystallization	Smectic
6	158.4	167.6	144.1	164.5
7	153.4	168.5	142.3	166.0
8	149.6	172.0	137.3	168.7
9	145.4	171.6	134.3	168.8
10	143.0	171.1	129.6	169.0
11	140.3	170.3	128.8	166.7
12	138.5	169.5	127.8	167.0

decreased to 138.5°C ($2S_{12}$) with increase in chain length. In contrast to azo-mesogens, here the smectic phase transitions are visible for all the Schiff base ($2S_n$) compounds in the heating cycle also. The smectic phase window is increased from 9.2°C (n = 6) to 31.0°C (n = 12). Similarly in the cooling scan also the crystal to smectic phase transition at 144.1°C ($2S_6$) decreased to 127.8°C ($2S_{12}$) and the smectic phase window is also increased from 13.4°C (n = 6) to 39.2°C (n = 12) with increase in chain length.

Optical micrographs of $2S_{11}$ and $2S_{12}$ obtained during the cooling cycle are shown in Figure 6. The micrograph of $2S_{11}$ exhibited fan texture with spherulitic domains at 131.4°C and crystal texture at 119.4°C similarly the micrograph of $2S_{12}$ exhibited fan texture with spherulitic domains at 142°C and crystal texture at 116.8°C. Further analysis of the mesophases was performed with X-ray diffraction.

As a representative case of Schiff's base dimesogens, an X-ray diffraction study was carried out on $2S_{12}$ to prove the presence of smectic phases beyond doubt. Figure 7 shows the X-ray diffractograms

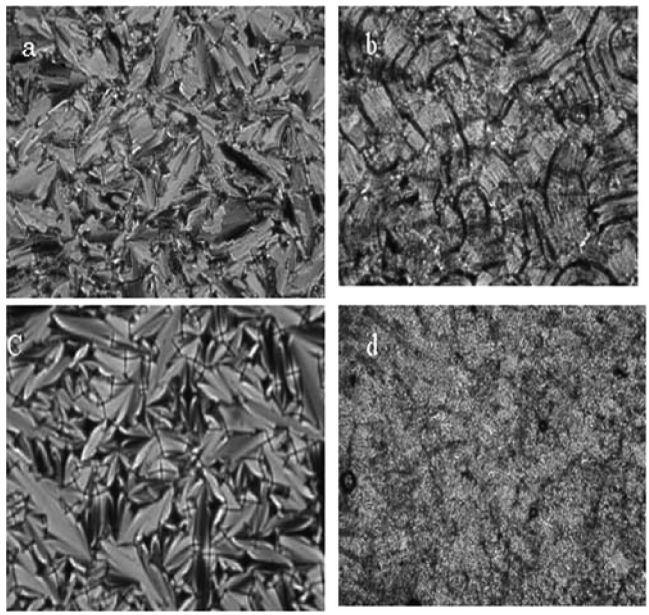

FIGURE 6 Optical photomicrographs of $2S_n$ (a) fan texture with spherulitic domains (Sm, cooling, 131.4°C), (b) crystal texture (Cr, cooling, 119.4°C) of $2S_{11}$ and (c) fan texture with spherulitic domains (Sm, cooling, 142°C), (d) crystal texture (Cr, cooling, 116.8°C) of $2S_{12}$ (10°C/min, ×100).

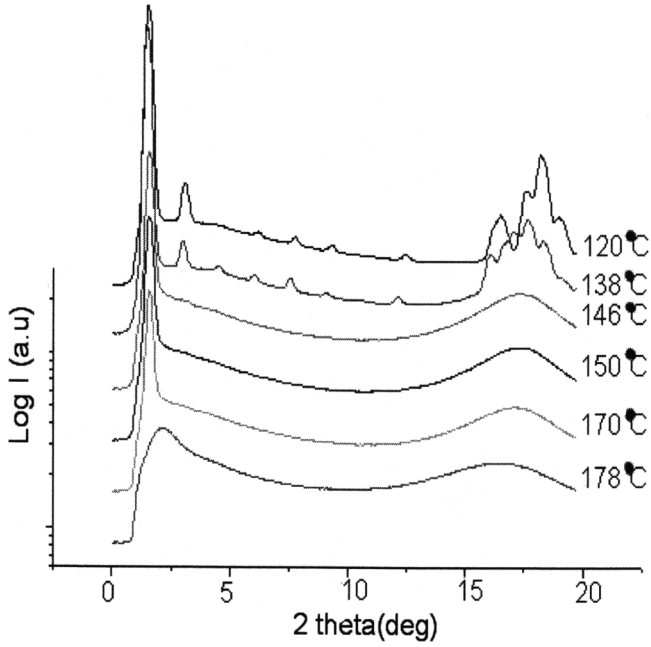

FIGURE 7 X-ray diffraction curves of Schiff base dimesogen ($2S_{12}$).

obtained at various temperatures for $2S_{12}$. It shows one sharp reflection at 120°C and 138°C in the small angle region and an array of small peaks in the wide angle regions corresponding to the formation of crystalline and various smectic phases. With increase in temperature, at 146, 150, and 170°C reflections corresponding to the smectic phases diffused, finally at 178°C, the crystalline phase also diffused and changed to isotropic liquid state. The sharp reflection in the small angle region confirms the formation of a highly ordered smectic A phase. In addition, small peaks, most probably a second order diffraction is seen in only at 120 and 138°C diffractograms of the compound in the liquid crystalline phase.

4. CONCLUSIONS

New series of symmetric azo and imine liquid crystal dimesogens have been prepared by varying terminal alkoxy chain length (n = 6–12) with a short spacer unit in between two mesogens. The chemical structures of these two series of dimesogens were examined by FT-IR and ^{1}H NMR spectroscopy. The mesomorphic properties and optical

textures of the resultant dimers were characterized by DSC, POM and XRD. The change in terminal alkoxy chain length has pronounced effect on the temperature range of smectic phase. In the DSC cooling scan, the smectic phase window of azo compounds increased from 6.4°C ($2A_6$) to 16.0°C ($2A_{12}$), whereas in Schiff base compounds, it increased from 9.2°C ($2S_6$) to 31.0°C ($2S_{12}$). Further, the $2A_{11}$ dimer was found to undergo photo induced configurational changes.

REFERENCES

[1] Imrie, C. T. (1999). *Struct. and Bond*, *95*, 149.
[2] Date, R. W., Imrie, C. T., Luckhurst, G. R., & Seddon, J. M. (1992). *Liq. Cryst.*, *12*, 203.
[3] Attard, G. S., Date, R. W., Imrie, C. T., Luckhurst, G. R., Roskilly, S. J., Seddon, J. M., *et al*. (1994). *Liq. Cryst.*, *16*, 529.
[4] Ikeda, T. (2003). *J. Mater. Chem*., *13*, 2037.
[5] Urbas, A., Tondiglia, V., Natarajan, L., Sutherland, R., Yu, H., Li, J. H., & Bunning, T. (2004). *J. Am. Chem. Soc*., *126*, 13580.
[6] Ichimura, S., Oh, S. K., & Nakagawa, M. (2000). *Science*, *288*, 1624.
[7] Komitov, L., Ichimura, K., & Strigazzi, A. (2000). *Liq. Cryst*., *27*, 51.
[8] Komitov, L., Ruslim, C., Matsuzawa, Y., & Ichimura, K. (2000). *Liq. Cryst.*, *27*, 1011.
[9] Yang, Y., Li, H., Wang, K., & Wen, J. (2001). *Liq. Cryst*., *28*, 375.
[10] Kelker, H. & Scheurle, B. (1969). *Angew Chem*., *81 922*, 903.
[11] So, B.-K., Jang, M.-C., Park, J.-H., Lee, K.-S., Song, H. H., & Lee, S.-M. (2002). *Opt. Mater.*, *21*, 685.
[12] So, B.-K., Kim, H.-J., Lee, S.-M., Song, H. H., & Park, J. H. (2006). *Dyes Pigments*, *70*, 38.
[13] So, B.-K., Kim, Y. S., Choi, M. M., Lee, S. M., Kim, J. E., Song, H. H., & Park, J. H. (2004). *Liq. Cryst*., *31*, 169.
[14] So, B.-K. (2001). Ph. D. Thesis. Hannam University, Daejeon, Korea.